COIN VIBRATION ANALYSIS IN CLASSICAL AND MINDLIN THEORY

EMIL VINTELER

Abstract. We studied 83 coins that belong to moderately thick circular plates with thickness *h* and radius *a* in the range $4.37 \leq a/h \leq 9.94$. The computed values in classical thin plate and first-order shear deformation Mindlin theory overestimate and respectively underestimate the experimental values for natural frequencies of coins. The Mindlin theory approximates better the experimental frequencies having the RMS value of 0.546 lower than the RMS value of 0.630 of the classical theory. The main uncertainty related to the values of the Young modulus and Poisson ratio of the studied alloys is resolved in this article by extracting them from the first two natural frequencies. The experimental frequencies of the studied coins can be used as a benchmark to compare the first-order with higher-order shear deformation theories. The study can be relevant to discriminate the coins in the vending machines with acoustic sensor.

Key words: vibration, eigenfrequency, circular plate, elasticity.

1. INTRODUCTION

Counterfeiting is a major economic problem [1]. Passed counterfeit currency (banknotes and coins) received by US domestic sources was 102 billion $ in 2023 [2]. 467.000 counterfeit banknotes with a value of 2.5 billion euro and 480.371 counterfeit euro-coins with a value of 0.9 billion € were detected in circulation in 2023 [3]. One criminal network linked to Camorra group produced and distributed 3 million counterfeit banknotes that represents one quarter of all counterfeit euro banknotes detected in circulation since the introduction of the euro [4]. A number of 4.07 billion of counterfeit euro-coins were detected from their introduction in 2002 [5].

The experimental characterization of antic coins is performed with scanning electron microscope, X-Ray fluorescence [6–7] and cathode-luminescence [8]. These experimental methods are slow and costly. All vending machines around world indentify the coins using low cost mechanical (measure diameter *d*, thickness

“Babeș-Bolyai” University, Cluj-Napoca, Romania, Physics Department

Ro. J. Techn. Sci. – Appl. Mechanics, Vol. 70, N^{os} 1–3, P. 81–96, Bucharest, 2025

DOI:10.59277/RJTS-AM.2025.1-3.05

h and weight *m*) or electromagnetic methods (measure material composition: density ρ, Young modulus *E* and Poisson ratio ν). These machines use methods based on coin image processing [9], electric conductivity [10], eddy current sensor [11–14] or acoustic sensor [15–16]. Due to the increase in counterfeiting sophistication, the new low cost methods of coin identification are based primary on acoustic resonance authentication that measure the natural frequencies of coin vibrations [17]. The natural frequencies were used to identify genuine coins in Europe [14–15], Japan [16], USA [18], counterfeited gold coins [19], ancient coins [20], coin flip [21–23]. Also the acoustic resonance testing for coins can be used as a learning tool [24] at undergraduate level to introduce basic notions in elasticity such as sound velocity in metals, Young modulus and Poisson ratio.

The computation of natural frequencies for vibration of circular plates can be performed analytically using the classical theory for thin plates [25] or the Mindlin theory [26–27] for moderately thick plates. Also the finite element analysis (FEA) [18] was used, but there was a large amount of error when comparing the simulated value of natural frequencies with the experimental ones for US coins. One explanation [18] was that the minting introduces a lot of strain hardening and the value of coin's Young modulus differs from the tabulated value of Young modulus for the same alloy. Another explanation [24] is that, due to the signs on the coin, the thickness *h* of coin is accurate only on the rim and to get a smaller difference between the simulated and experimental values of natural frequencies is better to introduce an effective thickness $h' = m/(\pi d^2/4)$. Another experimental source of errors is due to the fact that the majority of coins have a splitting of the fundamental vibration, hence appears the question to what experimental value of natural frequency is compared the simulated one. In article [19] the splitting of the fundamental vibration was attributed to the fact that coins are not flat disks, but such supposition was eliminated, because it was observed a variation in splitting for visually indistinguishable coins that have the same mark on their faces [24]. The classical theory for thin plates cannot predict this splitting. The majority of coins have some kind of plating, but it seems that only the higher frequency ranges are sensitive to the material at the surface of the coin. The lower frequency ranges tend to take into account the core material properties and it might be that the splitting of the fundamental vibration is due to the creation of micro cracks in the core of the coin after minting.

As far as we know only the classical thin plate theory was applied to compute the natural frequencies of euro-coins [15] and US coins [24]. It appears the question if the gap between theory and experiment is due to the specificity of these coins or the classical theory is not enough accurate. To solve this question we apply in this article the Mindlin theory that takes into account the coin thickness and in principle is more accurate. On the experimental part of the problem we use not only euro-coins and US coins, but a total of 83 coins with different diameter and thickness that are made from different alloys. Also we use the Young modulus and Poisson ratio values derived from experiment, and not the tabulated values for the coin alloy. The coin density is computed based on the alloy composition given by mint authorities of different countries.

2. METHODS

The natural frequencies f of coins as circular plates depend on the geometrical factor $G = h / \left(\pi\sqrt{3d^2} \right)$, where: d, h – coin diameter, respectively coin thickness, and the metal factor – P-wave – contraction wave velocity $V^2 = E / (\rho(1-\upsilon^2)$, where: E, ρ, υ – coin's Young modulus, density, respectively Poisson ratio:

$$f_{sn} = \Lambda_{sn}{}^2 GV \tag{1}$$

In the classical theory [25] the numerical factor Λ_{sn} has a slight dependency on Poisson ratio υ and the indices s and n refer to radial and azimuthally modes. It is known that for higher frequency modes of circular plates the experimental value diverge more from the theoretical value. The Mindlin theory [26–27] is used to remedy this problem for thick coins. The natural frequencies in the Mindlin theory satisfy the same relation (1), but the numerical factor Λ_{sn} depends on Poisson ratio υ and relative thickness $2h/d$. Mindlin [26–27] obtained the frequency of fundamental mode for free edge boundary condition. In [28] were obtained the frequencies of all modes for free edge, simply supported edge and clamped circular plates. Unfortunately their relations have several errors. Because this, we correct their relations and re-derive them from the conservation of linear momentum for the unit volume of a deformed body [29]:

$$\text{grad }(\sigma)+\rho f \ = \rho\partial_t{}^2 u \tag{2}$$

where *grad*, σ, ρ, f, t, u is the gradient operator, the stress tensor, the density of un-deformed body, the external force per unit mass, time and respectively the deformation vector. In the cylindrical coordinate system (r, θ, z) the gradient operator is $grad = (\partial/\partial r, (1/r)\partial/\partial\theta, \partial/\partial z)$ and equation (2) becomes:

$$\begin{gathered}
\sigma_{rr,\,r} + \sigma_{r\theta,\,\theta} / r + \sigma_{rz,\,z} + \left(\sigma_{rr} - \sigma_{\theta\theta}\right) / r + \rho f_r = \rho\, \partial_t{}^2 u_r, \\
\sigma_{r\theta,\,r} + \sigma_{\theta\theta,\,\theta} / r + \sigma_{\theta z,\,z} + 2\sigma_{r\theta} / r + \rho f_\theta = \rho\, \partial_t{}^2 u_\theta, \\
\sigma_{rz,\,r} + \sigma_{\theta z,\,\theta} / r + \sigma_{zz,\,z} + \sigma_{rz} / r + \rho f_z = \rho\, \partial_t{}^2 u_z,
\end{gathered} \tag{2a}$$

with $\sigma_{ij,k}=\partial u_{ij} /\partial x_k$.

For small deformations the strain tensor is expressed in terms of the deformation vector u:

$$\varepsilon = (1/2)\cdot\left(\text{grad }(u) + \left(\text{grad }(u)\right)^{\mathrm{T}} \right) \tag{3}$$

In the cylindrical coordinate system the strain components are:

$$\begin{gathered}\varepsilon_{rr} = u_{r,r},\ \varepsilon_{\theta\theta} = \left(u_r + u_{\theta,\theta}\right)/r,\ \varepsilon_{zz} = u_{z,z},\\ \varepsilon_{r\theta} = (u_{r,\theta}/r + u_{\theta,r} - u_\theta/r)/2,\\ \varepsilon_{rz} = \left(u_{r,z} + u_{z,r}\right)/2,\ \varepsilon_{\theta z} = (u_{z,\theta}/r + u_{\theta,z})/2,\end{gathered} \tag{3a}$$

with $u_{i,j} = \partial u_i/\partial x_j$.

For homogenous and isotropic materials the Hooke's law expresses the stress tensor σ in terms of the strain tensor:

$$\sigma = 2\mu\varepsilon + \lambda I \text{ trace } (\varepsilon), \tag{4}$$

where I is the unit matrix and the μ and λ are the Lame parameters for plane stress conditions can be expressed in terms of the Young modulus E and the Poisson ratio ν: $\lambda = E\,\nu/(1-\nu^2)$, $\mu = E/(2(1+\nu))$.

Using the eqs. (4) and (3a) the stress components in the cylindrical coordinate system are:

$$\begin{gathered}\sigma_{rr} = (\lambda+2\mu)[u_{r,r} + \nu(u_r/r + u_{\theta,\theta}/r + u_{z,z})],\\ \sigma_{\theta\theta} = (\lambda+2\mu)[(u_r + u_{\theta,\theta})/r + \nu\left(u_{r,r} + u_{z,z}\right)],\\ \sigma_{zz} = (\lambda+2\mu)[u_{z,z} + \nu(u_{r,r} + u_r/r + u_{\theta,\theta}/r)],\\ \sigma_{r\theta} = \mu(u_{r,\theta}/r + u_{\theta,r} - u_\theta/r),\quad \sigma_{rz} = \mu\left(u_{r,z} + u_{z,r}\right),\\ \sigma_{\theta z} = \mu(u_{z,\theta}/r + u_{\theta,z}),\end{gathered} \tag{4a}$$

with $\lambda + 2\mu = E/\left(1-\nu^2\right)$, $\lambda/(\lambda + 2\mu) = \nu$.

In the Mindlin theory [26–27] the deformation components have a linear dependence on z: $u = (z\,\psi_r, z\,\psi_\theta, W)$, where the new displacement functions ψ_r, ψ_θ and W in radial, angular and respectively normal to plate direction depend only on cylindrical components r, θ and on time t. Also the stress components have a linear dependence on z:

$$\begin{gathered}\left(\sigma_{rr}, \sigma_{\theta\theta}, \sigma_{r\theta}\right) = z\,(\lambda + 2\mu)\left(S_r, S_\theta, S_{r\theta}(1-\nu)/2\right),\\ \left(\sigma_{rz}, \sigma_{\theta z}\right) = \mu\left(S_{rz}, S_{\theta z}\right),\ \sigma_{zz} = z\,\lambda\,S_{zz},\\ S_r = \psi_{r,r} + \nu(\psi_r + \psi_{\theta,\theta})/r,\ S_\theta = (\psi_r + \psi_{\theta,\theta})/r + \nu\psi_{r,r},\\ S_{r\theta} = \psi_{r,\theta}/r + \psi_{\theta,r} - \psi_\theta/r,\ S_{rz} = \psi_r + W_{,r},\\ S_{\theta z} = \psi_\theta + W_{,\theta}/r,\ S_{zz} = \psi_{r,r} + \psi_r/r + \psi_{\theta,\theta}/r.\end{gathered} \tag{4b}$$

The moments and shearing forces are:

$$\begin{gathered}\left(M_r, M_\theta, M_{r\theta}\right) = \int_{-h/2}^{h/2}\left(\sigma_{rr}, \sigma_{\theta\theta}, \sigma_{r\theta}\right) z\,\mathrm{d}z =\\ = D\left(S_r, S_\theta, S_{r\theta}(1-\nu)/2\right)\left(Q_r, Q_\theta\right) =\\ = \int_{-h/2}^{h/2}\left(\sigma_{rz}, \sigma_{\theta z}\right)\mathrm{d}z = k^2 Gh\left(S_{rz}, S_{\theta z}\right),\end{gathered} \tag{5}$$

where h is the circular plate thickness, $D = Eh^3/\left(12\left(1-\nu^2\right)\right)$, $k^2 = \pi^2/12$, $G = \mu$ is the bulk shearing modulus.

The equations of motion for Mindlin circular plates are obtained by multiplying by z the first two equations (2a) and integrating all three equations (2a) by z from $-h/2$ to $h/2$ (in addition σ_{zz} is taken to be null):

$$\begin{aligned} &M_{r,r} + M_{r,\theta}/r + \left(M_r - M_\theta\right)/r - Q_r = \left(\rho h^3/12\right)\partial_t{}^2\psi_r, \\ &M_{r\theta,r} + M_{\theta,\theta}/r + 2M_{r\theta}/r - Q_\theta = \left(\rho h^3/12\right)\partial_t{}^2\psi_\theta, \\ &Q_{r,r} + Q_{\theta,\theta}/r + Q_r/r = (\rho h)\,\partial_t{}^2 W. \end{aligned} \tag{6}$$

Mindlin [26–27] obtained a solution for the equations of motion (6):

$$\begin{aligned} (\psi_r, \psi_\theta, W) = (&\left(s_1-1\right)w_{1,r} + \left(s_2-1\right)w_{2,r} + w_{3,\theta}/r, \\ &\left(s_1-1\right)w_{1,\theta}/r + \left(s_2-1\right)w_{2,\theta}/r - w_{3,r}/r, w_1 + w_2), \end{aligned} \tag{7}$$

that can be expressed in terms of three functions w_i that depend on trigonometric functions of angle θ, Bessel functions of first kind J_n of radius r and exponents of time t:

$$\begin{aligned} \left(w_1, w_2, w_3\right) = (&A_1 J_n\left(d_1 r/a\right)\cos(n\theta), A_2 J_n\left(d_2 r/a\right)\cos(n\theta), \\ &A_3 J_n\left(d_3 r/a\right)\sin(n\theta))\exp(i\omega t), \end{aligned} \tag{8a}$$

where A_i – arbitrary constants and the parameters s_i and d_i are:

$$\begin{aligned} &R = \left(h/a\right)^2/12,\ S = D/\left(Gh\left(ka\right)^2\right) = \left(h/a\right)^2 2/(\pi^2(1-\nu)), \\ &\Lambda^4 = \rho h a^4\omega^2/D,\ Q = R\Lambda^4 - 1/S,\ \left(s_1, s_2\right) = \left(d_2{}^2/Q, d_1{}^2/Q\right), \\ &d_1{}^2, d_2{}^2 = (\Lambda^4/2)[R + S \pm (\left(R-S\right)^2 + 4\Lambda^{-4})^{1/2}], \\ &d_3{}^2 = 2Q/(1-\nu), \end{aligned} \tag{8b}$$

depend on relative thickness h/a and frequency parameter Λ. For values of frequency parameter $\Lambda^4 < 1/(RS)$ the parameters d_2 and d_3 become imaginary and the Bessel functions $J_n(d_2r/a)$, $J_n(d_3r/a)$ should be replaced with the modified Bessel function $I_n(d_2r/a)$, $I_n(d_3r/a)$.

For coins with free edge condition we must impose the following constraints on the moments and shear forces for radius $r = a$:

$$M_r = M_{r\theta} = Q_r = 0. \tag{9}$$

Inserting the solution (7) for moments and shearing forces M_r, $M_{r\theta}$, Q_r in relations (5) the free edge condition (9) can be written in terms of parameters s_i and Bessel functions of first kind J_n with arguments d_i. The parameters s_i and d_i depend on frequency parameter Λ_{sn}. The free edge condition (9) is a homogenous liniar system of three equations with three unknowns A_i (introduced in relation (8a)) and nine coefficients C_{ij}

that depend only on the frequency parameter Λ_{sn}. We have a non-trivial solution for A_i only if det $(C_{ij}) = 0$ where the 3×3 matrix C_{ij} has the elements:

$$\begin{aligned}
&C_{1i} = (s_i - 1)(d_i^2 J_n''(d_i) + \nu K_i), C_{2i} = -2n(s_i - 1)L_i, \\
&C_{3i} = s_i d_i J_n'(d_i),\ i = 1,2, \\
&C_{13} = n(1-\nu)L_3, C_{23} = -d_3^2 J_n''(d_i) + K_3, C_{33} = nJ_n(d_3), \\
&K_i = d_i J_n'(d_i) - n^2 J_n(d_i),\ L_i = d_i J_n'(d_i) - J_n(d_i), \\
&\qquad i = 1,2,3.
\end{aligned} \tag{10}$$

The frequency factor Λ_{sn} (for fixed n, corresponding to Bessel function $J_n(x)$ and their derivatives $J_n'(x)$ and $J_n''(x)$, several solutions labeled by s exist) obtained from relation (10) depends on Poisson ratio υ and relative thickness h/a.

As an example, inserting in equation (10) the values from table 3 for the coin with number 78 (m = 31.10g, d = 40.60mm, ρ = 10.5g/cm^3, E = 77.9GPa, υ = 0.333) we obtain the following values for the frequency factor $\Lambda_{02} = 5.154$, $\Lambda_{10} = 8.898$, $\Lambda_{03} = 11.763$, $\Lambda_{11} = 19.542$, $\Lambda_{04} = 20.222$ for the first five modes. Inserting these values in equation (7) the deformation functions $W_{sn}(r, \theta)$ are obtained and their contour plots are represented in Fig. 1. The number n indicates the number of nodal diameters and s is the number of nodal circles.

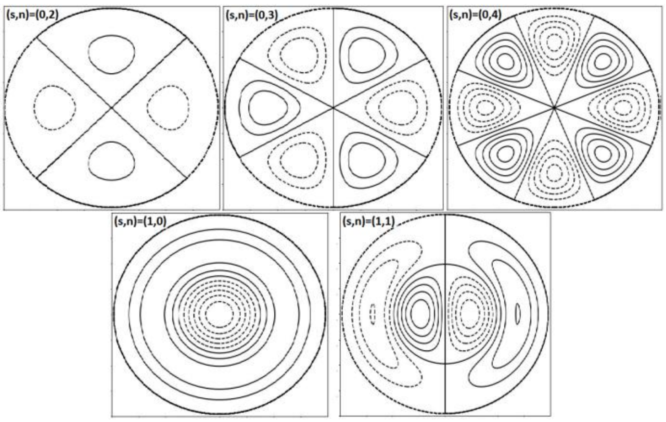

Fig. 1 – The contour plot of the deformation functions $W_{sn}(r, \theta)$ for the first five vibrational modes (s,n) = (0,2), (0,3), (0,4), (1,0), (1,1) of a free edge coin (the continuous lines and dashed lines are for positive and respectively negative values).

The frequency values f_{sn} of natural vibrations of coins are obtained from relation (1). In our computation we replace the thickness h with the effective thickness h' as was already made in the classical theory [24]. For our example with the coin with number 78 inserting the frequency factors Λ_{sn} in relation (1) we obtain the following first natural frequencies of this coin in the audible spectrum: f_{02} =3.80 kHz, f_{10} =6.56 kHz, f_{03} = 8.68 kHz, f_{11} =14.41 kHz, f_{04} =14.92 kHz.

The classical theory is recovered in the limit when the thickness h goes to zero and the free edge constraint det $(C_{ij}) = 0$ applies to 2×2 matrix C_{ij} with the elements C_{ij} ,i,j=1,2 given by relations (10) with parameters (8b) $R = 0 = S$, $s_1 = 0 = s_2$, $d_1 = \Lambda$, $d_2 = i\Lambda$:

$$\begin{aligned} C_{11} &= -\Big[\Lambda^2 J_n''(\Lambda) + \nu\big(\Lambda J_n'(\Lambda) - n^2 J_n(\Lambda)\big)\Big], \\ C_{12} &= -[\Lambda^2 I_n''(\Lambda) + \nu(\Lambda I_n'(\Lambda) - n^2 I_n(\Lambda))], \\ C_{21} &= 2n[\Lambda J_n'(\Lambda) - J_n(\Lambda)], \quad C_{22} = 2n[\Lambda I_n'(\Lambda) - I_n(\Lambda)], \end{aligned} \tag{11}$$

with $I_n(\Lambda) = J_n(i\,\Lambda)$ – the modified Bessel function of first kind. Introducing in equation (11) the values from Table 3 for the coin with number 78 (m = 31.10g, d = 40.60mm, ρ = 10.5g/cm^3, E = 74.9GPa, υ = 0.332) we obtain the following values for the frequency factor Λ_{02} = 5.255, Λ_{10} = 9.073, Λ_{03} = 12.231, Λ_{11} = 20.516, Λ_{04} = 21.506. Inserting the frequency factors Λ_{sn} in relation (1) the natural frequencies of the coin in classical theory in the audible spectrum are:

f_{02} =3.80 kHz, f_{10} =6.56 kHz, f_{03} = 8.84 kHz, f_{11} =14.83 kHz, f_{04} =15.55 kHz.

3. RESULTS AND DISCUSSIONS

In this article are studied the vibrations of 83 coins made from different alloys (containing predominantly steel, aluminum, zinc, copper, silver, gold) by bouncing them repeatedly on a hard surface. The sound is produced by the coin and surface vibration. It is useful to choose a surface with high elastic amortization [24]. Also the silver and gold coins can be held at the center with a pincer and gently stricken with another coin (ping method). The sound is recorded by a Smartphone at 48 kHz rate. The application Spectroid [30] using the Fast Fourier Transform obtains the natural vibrations of coins up to 24 kHz.

In all studied cases, for frequencies lower than 24 kHz, the corresponding number of natural vibrations is at most five. For coins made from steel and aluminum we have usually only the fundamental mode. The mints of different countries give the coin diameter and thickness and alloy composition; hence it is possible to use the available density and Poisson ratio of these alloys. The Young modulus of the alloy is also available, but in most cases its value is different from that obtained from the frequency. It is reasonable to suppose that the alloy elastic properties were modified due to coin minting.

In the study [24] was observed that the coins are not flat disks and is reasonable to replace in relation (1) the thickness h with an effective thickness $h' = m/(\pi\ \rho\ d^2/4)$. In this article we follow this replacement and the natural frequencies of coins depend only on the diameter d, mass m and its alloy composition (E, ρ, υ). In the Table 1 are 30 coins from aluminum, steel and copper alloys (in Appendix is given the country of provenience and the coin denomination) for which from the frequency of fundamental mode was computed the Young modulus within the classical circular thin plate theory. Coins with number 20 and 23 are bimetallic.

Table 1

Coins made from aluminum, steel and copper alloys with the frequency f_{sn} (kHz) for vibration mode (s,n) = (0,2) (due to splitting in some cases are two experimental values for the same theoretical mode (s,n)), coin mass m (g), diameter d (mm), density ρ (kg/m^3), Young modulus E (GPa), Poisson ratio υ

Coin	Composition	(0,2)	*m*	*d*	ρ	*E*	υ
1.10gr (A)	Al98.5Mg1.5	16.59,16.97	1.10	20.00	2678	66.7	0.32
2.1000L (RO)	Al97Mg3	20.19,20.83	2.00	22.20	2656	67.8	0.32
3.5000L (RO)	Al97Mg3	19.09,19.65	2.52	23.50	2656	60.1	0.32
4.500L (RO)	Al97Mg3	20.86,21.34	3.75	25.00	2656	52.8	0.32
5.10hr (UA)	Zn95Ni5	13.87	6.40	23.50	7211	91.9	0.25
6.1b (RO)	Fe95Cu5	23.19	2.40	16.75	7898	164.7	0.3
7.5b (RO)	Fe95Cu5	20.70,21.36	2.78	18.25	7898	200.5	0.3
8.2€c (E)	Fe95Cu5	20.16,20.96	3.06	18.75	7898	196.3	0.3
9.1¢ (US)	Fe95Zn5	16.90,17.00	2.50	19.05	7811	219.6	0.3
10.1p (GB)	Fe95Cu5	15.94,16.59	3.56	20.30	7898	171.3	0.3
11.10b (RO)	Fe95Ni5	18.80	4.00	20.50	7897	196	0.3
12.5L (RO)	Fe95Ni5	14.16,14.24	3.30	21.00	7898	199.4	0.3
13.1st (SK)	Fe95Cu5	16.32,16.50	3.85	21.00	7898	195.6	0.3
14.5€c (E)	Fe95Cu5	15.09	3.92	21.25	7898	175.4	0.3
15.2kc (CZ)	Fe95Ni5	14.44	3.70	21.50	7898	198	0.3
16.2st (SK)	Fe95Ni5	14.16	4.40	22.50	7898	193.6	0.3
17.100ft (H)	Fe95Ni5	19.59,19.97	8.00	23.80	7898	179.2	0.3
18.10kc (CZ)	Fe95Cu5	16.50,17.16	7.62	24.50	7898	180.3	0.3
19.10p (GB)	Fe95Ni5	15.09	6.50	24.50	7898	199.2	0.3
20.1£ (GB)	Cu70Ni30+Cu75Zn20Ni5	18.47,19.59	8.75	23.43	8928	179.7	0.34
21.20kc (CZ)	Cu75Zn25	14.34,14.81	8.43	26.00	8410	92.6	0.3
22.1ft (H)	Cu75Zn21Ni4	14.53,15.19	2.05	16.30	8489	94.4	0.34
23.1€ (E)	Cu75Ni25+Cu75Zn20Ni5	14.15	7.50	23.25	8930	125.7	0.31
24.5p (GB)	Cu75Ni25	17.81	3.25	18.00	8930	139	0.34
25.20gr (PL)	Cu75Ni25	15.66	3.22	18.50	8930	133.5	0.3
26.2zl (PL)	Cu75Ni25	14.62	5.21	21.50	8930	151	0.34
27.10€c (E)	Cu89Al5Zn5Sn1	15.56,16.03	4.10	19.75	7909	98.7	0.31
28.20€c (E)	Cu89Al5Zn5Sn1	13.59	5.74	22.25	7909	96.7	0.31
29.50€c (E)	Cu89Al5Zn5Sn1	12.28,13.31	7.80	24.25	7909	92.5	0.31
30.50gr (A)	Cu91.5Al8.5	13.22	3.00	19.50	7472	99.7	0.34

It is observed that the fundamental mode (in classical theory the (0,2) mode) splits in two peaks with very near frequencies (0, 2) and (0, 2'). We observed only two coins with number 56 and 60 that have splitting also for the second mode (1, 0) (see Table 4). The average of the split frequencies was used to compute the coin's Young modulus *E*.

For coins having two modes under 24 kHz it is possible to obtain also the alloy's Poisson ratio from the ratio of these modes. Indeed the ratio of the first two modes depends only on Poisson ratio via the numerical factors: $f_{11} / f_{02} = \lambda_{11}^2(\upsilon) / \lambda_{02}^2(\upsilon)$. In the Table 2 are 23 coins from zinc, steel and copper alloys for which from the frequency of the first two modes was computed the Poison ratio and Young modulus within the classical circular thin plate theory. Coins with number 37, 38, 47 and 48 are bimetallic. Coin with number 46 is a special case in that the frequencies at 14.5 kHz and 19.12 kHz correspond to (1, 0) and (0, 3) modes within the classical theory. If, on contrary, they correspond to (0, 2) and (1, 0) modes the computed Poisson ratio is well below 0.2 far away copper nickel alloy value of 0.34.

Table 2

Coins made from zinc, steel and copper alloys with the frequency f_{sn} (kHz) for vibration modes (*s*,*n*) = (0,2), (1,0) (due to splitting in some cases are two experimental values for the same theoretical mode (s,n)), coin mass *m* (g), diameter *d* (mm), density ρ (kg/m^3), Young modulus *E* (GPa), Poisson ratio υ

Coin	composition	(0,2)	(1,0)	*m*	*d*	ρ	*E*	υ
31.1¢ (US)	Zn97.5Cu2.5	12.7,13	20.11	2.50	19.05	7176	93.2	0.21
32.10L (RO)	Fe95Ni5	13.8	23.05	4.65	23.00	7898	196	0.295
33.20L (RO)	Fe95Ni5	11.38,11.62	19.38	5	24.1	7884	171	0.305
34.1L (RO)	Fe95Ni5	11.44	19.22	5	24.6	7898	199.9	0.30
35.5st (SK)	Fe95Ni5	12.00	20.25	5.4	24.75	7898	199	0.305
36.5ft (H)	Cu75Zn21Ni4	10.59,11.62	19.12	4.2	21.2	8489	102.4	0.33
37.2€ (E)	Cu75Zn20Ni5+ Cu75Ni25	10.31	17.53	8.50	25.75	8509	102	0.315
38.50kr (TR)	Cu75Zn10Ni15 +Cu81Zn15Ni4	11.72	20.06	7.00	23.85	8714	113.3	0.32
39.2ft (H)	Cu75Ni25	12.84	21.47	3.10	19.20	8930	130	0.295
40.50p (D)	Cu75Ni25	10.97,12.75	19.22	3.50	20.00	8930	118.1	0.255
41.50gr (PL)	Cu75Ni25	12.94	21.65	3.94	20.50	8930	138	0.295
42.5¢ (US)	Cu75Ni25	11.76,14.81	21.07	5.00	21.21	8930	114.6	0.23
43.1zl (PL)	Cu75Ni25	10.31	17.72	5.00	23.00	8930	138.8	0.325
44.1m (D)	Cu75Ni25	9.47,10.31	16.78	5.50	23.50	8930	124.4	0.31
45.10p (GB)	Cu75Ni25	10.50,10.78	17.91	6.50	24.50	8930	143	0.30
46.10st (SK)	Cu75Ni25	14.25	19.12	6.60	26.50	8930	158	0.34
47.50kr (TR)	Cu81Zn15Ni4+ Cu75Zn10Ni15	11.44	19.69	6.80	23.85	8613	111	0.33
48.50kr (TR)	Cu81Zn15Ni4+ Cu75Zn10Ni15	9.47	15.75	5.56	23.85	8613	111.5	0.29
49.20p (GB)	Cu81Ni17	13.03,13.31	22.12	5.00	21.40	8933	125.7	0.30
50.1$ (US)	Cu88.5Zn6 Mn3.5Ni2	8.40,8.60	14.40	8.10	26.49	8747	103.8	0.31
51.1sc (A)	Cu91.5Al8.5	10.59	17.91	4.20	22.50	7472	101.2	0.31
52.10¢ (US)	Cu91.67Ni8.66	12.78	20.86	2.27	17.91	8937	136.1	0.265
53.1¢ (US)	Cu95Zn5	12.60,12.90	21.90	2.50	19.05	8829	181.7	0.325

For coins having at least three modes with frequencies lower than 24 kHz it is possible to verify how well it is satisfied the classical thin plate theory by comparing the predicted third mode (using the Young modulus and Poisson ratio obtained from the first two modes) with the experimental one. In Table 3 are presented only the Young modulus and Poisson ratio (the first and second value is obtained in classical thin plate theory, respectively within the thick plate Mindlin theory). It is observed that the values in the Mindlin theory are usually bigger than those in classical theory. Coins with number 60 and 61 are bimetallic.

Table 3

Coins with at least three vibration modes in audible spectrum, coin mass m (g), diameter d (mm), density ρ (kg/m^3), Young modulus E (GPa), Poisson ratio υ – classical thin plate simulation (first value) and Mindlin thick plate simulation (second value)

Coin	Composition	m	d	ρ	E	υ
54.50L (RO)	Fe95Cu5	5.90	26.10	7898	167.7,173.6	0.296,0.296
55.100L (RO)	Fe95Ni5	8.80	29.10	7898	190.7,198.2	0.307,0.309
56.5q (EG)	Cu70Zn30	3.20	21.00	8029	104.7,108.1	0.248,0.248
57.5k (HR)	Cu63.1Ni23.2Zn13.7	7.45	26.50	8633	119.9,125.0	0.324,0.325
58.500¥ (J)	Cu72Zn20Ni8	7.00	26.50	8508	104.3,108.5	0.334,0.335
59.20ft (H)	Cu75Zn21Ni4	6.90	26.30	8489	108.4,112.8	0.333,0.334
60.200ft (H)	Cu75Ni25+ Cu75Zn21Ni4	9.00	28.30	8930	130.5,135.5	0.317,0.318
61.1L (TR)	Cu75Zn10Ni15 +Cu81Zn15Ni4	6.65	26.15	8714	166.8,172.7	0.311,0.311
62.5sc (A)	Cu75Ni25	4.80	23.50	8930	122.4,126.4	0.242,0.242
63.10ft (H)	Cu75Ni25	6.10	24.80	8930	134.3,139.5	0.309,0.310
64.10sc (A)	Cu75Ni25	6.20	26.00	8930	140.7,145.1	0.332,0.333
65.5m (D)	Cu75Ni25	10.00	29.00	8930	132.5,137.9	0.3260.328
66.50b (RO)	Cu80Zn15Ni5	6.10	23.75	8612	102.5,107.9	0.331,0.334
67.25¢ (US)	Cu91.67Ni8.66	5.67	24.26	8937	129.3,134.2	0.294,0.295
68.1/2$ (US)	Cu91.67Ni8.66	11.34	30.61	8937	126.0,130.9	0.312,0.312
69.5gr (PL)	Cu95Zn5	2.59	19.50	8829	119.7,123.7	0.371,0.371
70.2p (GB)	Cu97Zn2.5Sn0.5	7.12	25.90	8874	116.2,120.9	0.321,0.323
71.wa (US)	Ag90Cu10	6.25	24.26	10155	74.5,77.1	0.277,0.277
72.wl (US)	Ag90Cu10	12.50	30.63	10155	73.7,76.6	0.405,0.407
73.mp (US)	Ag90Cu10	26.73	38.10	10155	74.7,78.1	0.344,0.345
74.ra (MC)	Ag90Cu10	30.00	41.00	10155	73.5,76.2	0.341,0.342
75.vi (A)	Ag	31.10	37.00	10500	69.1,73.5	0.324,0.329
76.ma (CA)	Ag	31.11	37.97	10500	68.7,72.6	0.356,0.360
77.br (GB)	Ag	31.21	38.61	10500	70.4,74.0	0.307,0.310
78.ea (US)	Ag	31.10	40.60	10500	74.9,77.9	0.332,0.333
79.25kr (TR)	Au91.67Cu8.33	1.75	18.00	17616	102.9,103.7	0.384,0.382
80.kr (SA)	Au91.67Cu8.33	33.93	32.77	17616	87.1,92.0	0.346,0.350
81.ea (US)	Au91.67Ag3Cu5.33	33.93	32.70	17772	77.8,82.5	0.387,0.391
82.ma (CA)	Au	31.10	30.00	19320	56.6,61.0	0.347,0.354
83.br (GB)	Au	31.10	32.69	19320	73.4,76.4	0.332,0.334

In Table 4 and Table 5 are presented the experimental values of natural vibrations vs. simulated values for coins with at least three vibration modes. For coin 56 the classical and Mindlin frequency values are smaller than the experimental one. It is possible that the alloy composition used in computation to be wrong. For all coins apart those with number 56, 60, 61, 64, 68, the frequency value within the Mindlin theory is lower than the experimental one underestimating it, while the classical theory value overestimates it.

Table 4

Coins from steel and copper alloys with the frequency f_{sn} (kHz) for vibration modes (s,n)=(0,2), (1,0), (0,3): experiment (first values – in some cases due to splitting are two values) *vs* classical thin plate simulation (second value) and Mindlin thick plate simulation (third value)

Coin	(0,2)	(1,0)	(0,3)
54.50L (RO)	9.61,9.93;9.77;9.77	16.36;16.36;16.36	22.39;22.67;22.29
55.100L (RO)	9.91,10.14;10.03;10.03	16.95;16.95;16.95	23.17;23.29;22.83
56.5q (EG)	9.37;9.37;9.37	14.81,15.37; 15.09;15.09	23.06;21.67;21.33
57.5k (HR)	8.53;8.53;8.53	14.62;14.62;14.62	19.69;19.83;19.43
58.500¥ (J)	7.38,7.86;7.62;7.62	13.18;13.18;13.18	17.51;17.73;17.40
59.20ft (H)	7.59,8.25;7.92;7.92	13.69;13.69;13.69	18.09;18.43;18.08
60.200ft (H)	7.12,8.62;7.87;7.87	12.47,14.34; 13.41;13.41	17.62;18.29;17.94
61.1L (TR)	9.37;9.37;9.37	15.88;15.88;15.88	21.28;21.76;21.37
62.5sc (A)	7.97, 9.47;8.72;8.72	13.97;13.97;13.97	20.16;20.15;19.83
63.10ft (H)	9.19;9.19;9.19	15.56;15.56;15.56	21.00;21.35;20.94
64.10sc (A)	7.87;7.87;7.87	13.59;13.59;13.59	17.9;18.32;18.01
65.5m (D)	7.97;7.97;7.97	13.69;13.69;13.69	18.66;18.54;18.16
66.50b (RO)	10.0210.02;10.02	17.29;17.29;17.28	23.24;23.32;22.73
67.25¢ (US)	9.12,9.24;9.18;9.18	15.35;15.35;15.35	20.97;21.30;20.91
68.1/2$ (US)	7.12;7.12;7.12	12.08;12.08;12.08	16.19;16.54;16.23
69.5gr (PL)	9.47,9.84;9.66;9.66	17.25;17.25;17.25	22.31;22.53;22.16
70.2p (GB)	8.44;8.44;8.44	14.44;14.44;14.44	19.12;19.63;19.22

It can be seen for several coins (with number 75, 76, 77, 79 and 82) that the experimental modes are absent even though the simulated ones are within the audible range under 24 kHz. It is possible that the amplitude of higher modes is smaller than the background noise, but also it is possible that the energy dissipation to be greater for higher modes (the dissipation is not taken in account in these theories).

It can also been observed that for higher modes the frequencies in Mindlin theory are lower than those in classical theory. For coin with number 72 (υ = 0.407) and 81 (υ = 0.391*)* due to the high value of Poisson ratio, the frequency value of (0, 4) mode vibration is lower than that of (1, 1) mode in Mindlin theory. This behavior does not occur in the classical theory, where the frequency value of (0, 4) mode vibration is always higher than that of (1, 1) mode for all coins.

Table 5

Coins from silver and gold alloys with the frequency f_{sn} (kHz) for vibration modes (s,n)=(0,2), (1,0), (0,3), (1,1),(0,4): experiment (first row – in some cases due to splitting are two values) *vs* simulation (second row) in classical thin plate theory (first value) and Mindlin thick plate theory (second value).

Coin	(0,2)	(1,0)	(0,3)	(1,1)	(0,4)
71.wa (US)	6.37 6.37,6.37	10.5 10.5,10.49	14.81 14.76,14.50	23.06 23.98,23.33	- 25.88,24.90
72.wl (US)	4.83 4.83,4.83	8.91 8.90,8.91	11.25 11.30,11.08	19.87 19.89,19.34	21.28 20.01,19.13
73.mp (US)	4.41 4.41,4.41	7.69 7.69,7.69	10.03 10.27,10.05	16.41 17.35,16.79	17.25 18.07,17.24
74.ra (MC)	3.66 3.66,3.66	6.37 6.37,6.37	8.34 8.53,8.37	14.34 14.38,14.00	14.81 15.00,14.41
75.vi (A)	5.30 5.30,5.30	9.09 9.09,9.09	12.00 12.33,11.97	-20.58,19.64	- 21.67,20.31
76.ma (CA)	4.73 4.73,4.73	8.34 8.34,8.34	10.87 11.03,10.73	18.94 18.78,18.01	- 19.42,18.30
77.br (GB)	4.55 4.55,4.55	7.69 7.69,7.69	10.41 10.56,10.31	14.90 17.46,16.82	- 18.55,17.60
78.ea (US)	3.80 3.80,3.80	6.56 6.56,6.56	8.72 8.84,8.68	14.43 14.83,14.41	15.20 15.55,14.92
79.25kr (TR)	2.95 2.95,2.95	5.34 5.34,5.34	6.75 6.90,6.87	11.70 11.97,11.90	- 12.17,12.05
80.kr (SA)	4.83 4.83,4.83	8.44 8.44,8.44	10.97 11.25,10.94	17.91 19.04,18.29	18.94 19.80,18.65
81.ea (US)	4.5 4.5, 4.5	8.16 8.16,8.16	10.41 10.51,10.23	17.16 18.27,17.50	18.00 18.54,17.45
82.ma (CA)	4.59,5.06 4.83,4.83	8.44 8.44,8.44	11.06 11.24,10.84	- 19.03,17.96	- 19.78,18.28
83.br (GB)	3.47,3.70 3.59,3.58	6.19 6.19,6.19	8.25 8.35,8.17	13.59 14.00,13.57	14.25 14.67,14.03

The Root Mean Square (RMS) for all differences between the experimental and simulation frequency values is 0.630 in the classical theory and a lower value of 0.546 in Mindlin theory. If we choose separately the (0, 3), (1, 1) and (0, 4) modes than these RMS are 0.373, 1.010 and 0.722 in classical theory and 0.376, 0.719, 0.791 in Mindlin theory. We expect a lower value for Mindlin theory for higher modes, but this happens only for the (1, 1) modes. The reason might be due to the small sets of higher modes, from 30 coins having (0, 3) modes only 11 coins have (1, 1) modes and only 7 coins have (0, 4) modes.

5. CONCLUSIONS

We studied experimentally the frequencies of natural coin vibrations for 83 coins made from different alloys. Within the classical circular thin plate theory for 30 coins with one vibration in the audible spectrum the Young modulus was computed and for 23 coins with two vibrations in the audible spectrum the Poisson ratio and Young modulus were computed. For remaining 30 coins with at least three vibrations in the audible spectrum, the Poisson ratio, Young modulus and the frequencies of the first five modes were computed, within the classical and Mindlin theory. The frequency value within Mindlin theory is lower than the experimental one underestimating it for 25 coins out of 30 coins with three vibrations in the audible spectrum, while the classical theory value overestimates it. The Mindlin theory approximates better the experimental frequencies having the RMS value of 0.546 lower than the RMS value of 0.630 of the classical theory.

Plates are classified [31] by the inverse of their relative thickness a/h as thick for a/h<5, moderately thick 5 < a/h <10, thin 10 < a/h < 50 and very thin 50 < a/h. The thin plates are well described by classical plate theory [25]. The moderately thick plates can be described by first order shear deformation theories, in particular by Mindlin theory [26–27]. Higher order shear deformation theories [32] can be used for thick plates and can improve the accuracy of higher modes frequencies for moderately thick plates. In article [33] is given the exact solution of 3D elasticity theory for circular plates, but unfortunately for two very specific boundary conditions: rigid slipping and elastic simple support. In article [34] is used the Reddy third-order shear deformation theory and in the study [35] is used the Ritz analysis for the higher order shear deformation theory. In these articles the free boundary condition can be imposed and the values of frequency factors can be compared with those obtained from the Mindlin theory.

The studied coins belong to moderately thick circular plates with 5.15 (1lira (GB) coin no. 20) $\leq a/h \leq$ 9.94 (10sc (A) coin no. 64) and only one coin is a thick circular plate with a/h = 4.37 (500L (RO) coin no. 4). In [35] it is shown that the factor frequency Λ_{10} and Λ_{11} in Mindlin theory are with 0.2% and respectively 0.4% lower than in the 3D exact theory of thick plate with Poisson ratio $\nu = 0.3$, $a/h = 5$ and free edge boundary condition. It also says that while Mindlin theory improves the values of factor frequencies compared to classical thin plate theory, it underestimates these values compared to 3D exact theory. This result is in accord with our result that the frequency values in Mindlin theory underestimate the experimental ones, while the classical theory values overestimate them. In [35] it is shown that also the values of factor frequency Λ_{02}, Λ_{03} and Λ_{04} in Mindlin theory are lower with 0.1%, 0.55% and respectively 0.35% with respect to those in 3D exact theory. The conclusion is that for our list of coins that are moderately thick circular plates the first five natural frequencies in Mindlin theory differ from those in the exact theory on average around 1%.

The measured frequencies for our list of coin can serve as a benchmark to test the first order and higher order shear deformation theories. The coins are circular plates with a high degree of standardization with small deviations in their geometric and material properties. This is reflected in small standard deviation of their natural frequencies. In [16] it was shown that for 300 coins the standard deviation is under 0.11 for the first four natural frequencies. However to serve as benchmark, the coins must have at least three frequencies in the audible spectrum.

The reason is that the tabulated values for the Young modulus and Poisson ratio for the alloys used in coins cannot be trusted and instead must be computed from the first two natural frequencies of the coins. The Young modulus can be obtained alternatively by measuring the sound velocity with an ultrasound pulse-echo [37]. The coins with at least three frequencies in the audible spectrum are very diverse with Poisson ratio and Young modulus in the range 0.242–0.407 and respectively 61–198.2 GPa. It is an interesting problem to see in what region of geometric and material parameters is the greatest deviation between experiment and first order and higher order shear deformation theories.

In this study the classical theory and the Mindlin theory were applied to isotropic and homogenous materials. The real coins are obtained by minting (cold pressing) hence there are internal strains and anisotropy between Young modulus values for in-plane and normal-to-plane directions. The real coins are also coated with a protective superficial layer obtained by electrolytic deposition that can modify their vibrations. The bimetallic coins (1lira GB (coin with number 20), 50 kc (21), 1euro (23), 2 zl (26), 2euro (37), 50kr (38) (47) (48), 500yen (58), 200ft (60), 1lira (61), 5 mark (65)) are not homogenous: they have an outer ring and a center made from different alloys. We approximated them with one material having intermediate values for Poisson ratio, density and Young modulus. The euro and new yens coins have also a center laminated in three sheets made from different alloys. In these cases we should apply the more general theory of laminated plates [38].

The polygonal coins with many faces (5000L (3) is a 12-faced polygon coin, 2kc (15) is a 11-faced polygon coin, 20 kc (21) is a 13-faced polygon coin, 20p (49) is a 7-faces polygon coin) are approximated well by circular plates, however it would be desirable to compare the frequencies with those obtained within the theory of polygonal plates [39].

One of the possible applications of the present study is the construction of coin-processing machine able to separate counterfeit coins from genuine euro coins [15, 16, 40]. It was shown in [16] that the first three natural frequencies can be used to separate in distinct regions the non-valid coins from the valid ones. An EU coin-processing machine must be able to separate the following sample of non-valid coins that appear in the ETSC – Guidelines [41]: dirty (with glue, oil stain, ink), oxidation, mechanically damaged, wrongly assembled, mint defects, burnt, polished and cleaned, altered coins for decorative or artistic purposes. In principle all modifications or deviations from the geometry of circular plate can affect the natural frequencies of coin vibration: holes, cuts, bent, polished or deformed surface, ring and separated coin core etc. But the frequencies are not affected by dirtiness, small corrosion or a thin layer of paint. Complementary methods and sensors are necessary to facilitate the exclusion of these categories of non-valid coins.

Received on July 19, 2025

REFERENCES

1. QUERCIOLI, E., SMITH, L., *The economics of counterfeiting*, Econometrica, **83**, *3*, pp. 1211–1236, 2015.
2. JUDSON, R., *Estimating the Volume of Counterfeit U.S. Currency in Circulation*, International Finance Discussion Papers 1404, Washington, Board of Governors of the Federal Reserve System, 2025.
3. BCE, *Number of counterfeit euro banknotes remains low in 2023*, European Central Bank Press Release 29 January, 2024.
4. EUROPOL, *The other side of the coin*, European financial and economic crime threat assessment 2023, European Union Agency for Law Enforcement Cooperation, 2023.
5. ETSC, *The protection of euro coins in 2023*, Situation as regards euro coin counterfeiting and the activities of the European Technical & Scientific Centre (ETSC), European Commission Report 8865144, 11 December, 2024.
6. CONSTANTINESCU, B., BUGOI, R., OBERLÄNDER-TÂRNOVEANU, E., PÂRVAN, K., *Some considerations on x-ray fluorescence use in museum measurements – the case of medieval silver coins*, Rom. Rep. Phys., **57**, *4*, pp. 1021–1031, 2005.
7. BROWN, J., *Counterfeit coins*, B.Sc. thesis, Brigham Young University, 2007.
8. PINGITORE, V., BARBERIO, M., OLIVA, A., NOCE, N., GATTUSO, C., DAVOLI, M., *Golden drachma from bruttìa: counterfeit money revealed by scanning electron microscopy and cathodoluminescence*, Med. Arch. Arch., **8**, *2*, pp. 31–38, 2008.
9. KHAZAEE, S., RAD, M.S., SUEN, C.Y., *Detection of counterfeit coins based on 3D height-map image analysis*, Expert Syst. Appl., **174**, 114801, 2021.
10. LASS, E.A., STOUDT, M.R., CAMPBELL, C.E., *Systems design approach to low-cost coinage materials*, Integr. Mater. Manuf. Innov., **7**, pp. 52–69, 2018.
11. LU, C.C., CHANG, W.L., WANG, C.C., YU, S.F., JENG, J.T., *A statistical pattern analysis approach for rapid coin identification based on Eddy-current sensors*, Procedia. Eng., **15**, pp. 5579–5583, 2011.
12. CARLOSENA, A., ALFONSO, A.J., ARIZTI, F., MARTINEZ-DE-GUERENU, A., *Sensing in coin discriminators*, In Proceedings of the IEEE Sensors Applications Symposium, San Diego, CA, USA , 6–8 February 2007, pp. 1–6.
13. DAO, D.V., JENG, J.T., DOAN, V.D., NGUYEN, H.T., LIANG, B.Y., Development of Electromagnetic Acoustic Transducer System for Coin Classification, Sensors, **22**, 9055, 2022.
14. GORDON, R., MÄRTENS, O., LAND, R., MIN, M., RIST, M., GAVRIJAŠEVA, A., POKATILOV, A., KOLYSHKIN, A., *Eddy current validation of Euro-coins, Lecture Notes on Impedance Spectroscopy*, Measurement, Modeling and Applications, **3**, Olfa Kanoun (Ed.), CRC Press, London, 2012.
15. GAVRIJASEVA, A., MARTENS, O., LAND, R., *Acoustic spectrum analysis of genuine and counterfeit euro coins*, Elektronika ir Elektrotechnika, **21**, *3*, pp. 59–57, 2015.
16. SUZUKI, M., *Development of a simple and non-destructive examination for counterfeit coins using acoustic characteristics*, Forensic science international, **177**, *1*, pp. e5–e8, 2008.
17. KRALJEVSKI, I., DUCKHORN, F., JU, Y., TSCHOEPE, C., RICHTER, C., WOLFF, M., *Acoustic Resonance Recognition of Coins*, 2020 IEEE International Instrumentation and Measurement Technology Conference, Dubrovnik, Croatia.
18. STEED, E., *Coin identification through natural frequency analysis*, Brigham Young University Report, 2015.
19. MANAS, A., *The music of gold: Can gold counterfeited coins be detected by ear?*, Eur. J. Phy. **36**, *4*, 045012, 2015.
20. JIN, X., WANG, X., CAO, X., XUE, C., *Construction and recognition of acoustic ID of ancient coins based on deep learning of artificial intelligence for audio signals*, Herit Sci., **11**, 46, 2023.
21. STEFAN, R.C., CHECHE, T.O., *Coin Toss Modeling*, Rom. Rep. Phys. **69**, 904, 2017.

22. CHANDRA, K., *Can One Hear the Fate of a Coin?*, Stanford Report, 2020.
23. BARTOS, F. *et al.*, *Fair coins tend to land on the same side they started: evidence from 350,757 flips*, arXiv:2310.04153v4, 2025.
24. RAKESTRAW, D., PAUL, P., *Resonant Acoustic Characterization of Coins: An Inquiry-Based Learning Activity for Everyone with a Smartphone*, Lawrence Livermore National Laboratory Report LLNL-TR-829101, 10 November 2021.
25. LEISSA, A.W., *Vibration of plates*, NASA report NASA SP-160, Washington DC, 1969.
26. MINDLIN, R.D., DERESIEWICZ, H., *Thickness-shear and flexural vibrations of a circular disk*, J. Appl. Phys., **25**, pp. 1329–1332, 1954.
27. DERESIEWICZ, H., MINDLIN, R.D., *Axially Symmetric Flexural Vibrations of a Circular Disk,* ASME J. Appl. Mech., **22**, pp. 86–88, 1955.
28. IRIE, T., YAMADA, G., AOMURA, S., *Natural frequencies of Mindlin circular plates*, Transactions of ASME J. Appl. Mech., **47**, pp. 652–655, 1980.
29. REDDY, J.N., *Theory and Analysis of Elastic Plates and Shells*, CRC Press, Boca Raton, 2006.
30. REINKE, C., *Spectroid – smartphone application for Android platform*, version 1.1.2., 6 June 2024.
31. SZILARD, R., *Theories and applications of plate analysis: classical, numerical and engineering methods*, John Wiley and Sons, New Jersey, 2004.
32. GHUGAL, Y.M., SHIMPI, R.P., *A Review of Refined Shear Deformation Theories of Isotropic and Anisotropic Laminated Plates*, J. Reinforced Plastics and Composites, **21**, pp. 775–813, 2002.
33. DING, H.J., XU, R.Q., CHI Y.W., CHEN W.Q., *Free axisymmetric vibration of transversely isotropic piezoelectric circular plates*, International Journal of Solids and Structures, **36**, *30*, pp. 4629–4652, 1999
34. HOSSEINI-HASHEMI, SH., ES'HAGHI, M., TAHER, H., FADAIE, M., *Exact closed-form frequency equations for thick circular plates using a third-order shear deformation theory,* Journal of Sound and Vibration, **329**, pp. 3382–3396, 2010.
35. LIEW, K.M., YANG, B., *Three-dimensional elasticity solutions for free vibrations of circular plates: A polynomials-Ritz analysis,* Comput. Methods Appl. Mech.Engrg., **175**, pp.189–201, 1999.
36. SO, J., LEISSA, A.W., *Three-dimensional vibrations of thick circular and annular plates*, Journal of Sound and Vibration, **209**, pp. 15–41, 1998.
37. PETRONYUK, Y. TITOV, S. LEVIN, V., *Application of acoustic microscopy for evaluation of numismatic material*, Journal of Physics: Conference Series, **2091**, 012045, 2021.
38. REDDY, J.N., *Mechanics of Laminated Composite Plates and Shells*, CRC Press, Boca Raton, 2004.
39. WANG, C.Y., *Vibrations of Completely Free Rounded Regular Polygonal Plates*, International Journal of Acoustics and Vibrations, **20**, pp. 107–112, 2015.
40. DIMITROV, D., KRASTEVA, J., GEORGIEV, G., *Possibilities to use the eigenfrequencies to identify coins*, Eastern Academic Journal, **2**, pp. 69–75, 2016.
41. ETSC Guidelines, On the implementation of Regulation (EU) No 1210/2010 of the European Parliament and of the Council of 15 December 2010 concerning authentication of euro coins and handling of euro coins unfit for circulation, Ref. Ares(2019)6661509 - 28/10/2019

Appendix. Country: A – Austria (gr – groschen, sc – schilling, vi – Vienna philarmonic), CA – Canada (ma – maple), CZ – Czech Republic (kc – koruna), D – Germany (p – phening, m – mark), E – Europe (€c – eurocent, € – euro), EG – Egypt (q – quirsh), GB – Great Britain (br – britannia, p – pence, £ – lira), H – Hungary (ft – forint), HR – Croatia (k – kuna), J – Japan, MC – Monaco (ra – 50 francs rainier), PL – Poland (gr – groszy, zl – zloty), RO – Romania (b – ban, L – lei), SA – South Africa (kr – krugerrand), SK – Slovakia (st – koruna), TR – Turkey (kr – kurus, L – lira), UA – Ukraine (hr – hryvnia), US – United States of America (¢ – cent, $ – dollar, ea – eagle, mp – morgan peace, wa – washington, wl – walking liberty)..